

One step method to encapsulate nanocatalysts within Fe₃O₄ nanoreactors†Shouhu Xuan,^{*a} Yufeng Zhou,^c Huajian Xu,^d Wanquan Jiang,^c Ken Cham-Fai Leung^{*b} and Xinglong Gong^{*a}

Received 17th June 2011, Accepted 3rd August 2011

DOI: 10.1039/c1jm12798e

Here reported a facile approach to synthesize rattle type magnetic nanocomposite with a permeable Fe₃O₄ shell and noble metallic core. The core of yolk materials are controlled by varying the metallic ion precursor (such as K₂PdCl₄, AgNO₃, KAuCl₄, and Cu(NO₃)₂). The content of the metallic cores increases by increasing of the amount of the metallic salt. This one step method is based on an *in situ* reduction and Ostwald ripening process. As-obtained particles show porous nature and superparamagnetic characteristic. Moreover, the as-prepared magnetic recyclable nanocatalyst manifests high activity when evaluated for their catalytic properties and they can be separated from the reaction system by using a magnet.

1. Introduction

Owing to their well-defined interior voids, low density, and large surface area, hollow micro/nanostructures have attracted growing research interests in a myriad of applications.^{1–4} If the shell is permeable to reactants, this hollow nanostructure can be considered in a wider sense as a tiny reactor while containing a movable catalyst core.^{5,6} Regarding their catalytic property, many works have been reported on developing such a rattle type nanostructure.⁷ Templating against various types of colloid particles is probably the most effective and general method for yielding nanorattles.^{8,9} Unfortunately, the core particle requires coating with double shells, rendering multistep and complex synthetic procedures. To solve this problem, Kirkendall effect,¹⁰ selective etching of the core particle,¹¹ shell sacrificed templating,¹² soft templating,¹³ and other methods were also exploited to synthesize nanorattles. However, these methods still require the preparation of core/shell templates.

The noble nanoparticles in the rattle structure could act as catalysts to carry out a wide range of reactions.¹⁴ To allow for the easy removal of catalysts from reaction mixtures, magnetic supports which contain magnetic nanoparticles, may be required

in this emerging area of research. In the past decades, many works were focused on immobilizing nanocatalysts on the surface of magnetic carriers.^{15,16} To improve the stability of the noble nanoparticles, porous shell was further covered on the surface of the magnetic nanocatalysts to protect the supported nanocatalysts.^{17,18} In this case, nanocatalysts confined within a magnetic porous carrier exhibit high catalytic activity and recyclability. Hollow magnetic particles with porous shells have been proven to be an ideal reservoir for noble nanoparticles.¹⁹ Apart from its normal role of magnetic driver, the hollow interior could also be considered as a nanoreactor.²⁰ The hollow shell can also protect the growth and aggregating of the metal core during catalytic reaction.²¹ Therefore, rattle type magnetic nanocatalysts are expected for the widespread industrial use.²²

The Ostwald ripening process was widely utilized for generation of hollow interiors for nanomaterials due to its nature of matter relocation.²³ By controlling the size distribution and aggregation patterns of the primary crystals, both hollow and core shell nanostructures can be obtained.^{24,25} Li and his colleague reported that this approach could also offer a method for the synthesis of yolk like nanostructure and the as-prepared hollow Au–TiO₂ core shell composites shown stable photocatalytic property.⁵ In recently, various methods have been developed to synthesize yolk shell particles and both anisotropic and isotropic structures were developed.^{26–28} However, the Ostwald ripening approach has not been applied for the synthesis of yolk-like magnetic nanocomposites. In addition, there is still a synthetic challenge in developing a general, facile, and scalable approach to fabricate porous magnetic hollow spheres with encapsulation of catalytic nanoparticles.

Herein, we report that rattle type noble metal@Fe₃O₄ nanocomposites with superparamagnetic characteristic and porous nature can be synthesized by using a simple one-step wet chemical approach. This method offers the flexibility in

^aCAS Key Laboratory of Mechanical Behavior and Design of Materials, Department of Modern Mechanics, University of Science and Technology of China, Hefei, 230026, P. R. China. E-mail: xuansh@ustc.edu.cn; Fax: +86 551 3606382; Tel: +86 551 3606382; gongxl@ustc.edu.cn; +86 551 3600419; +86 551 3600419

^bCenter of Novel Functional Molecules and Institute of Molecular Functional Materials, Department of Chemistry, Chinese University of Hong Kong, Shatin, NT, Hong Kong SAR, P. R. China. E-mail: cfleung@cuhk.edu.hk; Fax: (+852) 2603 5057; Tel: (+852) 2609 6342

^cDepartment of Chemistry, University of Science and Technology of China, Hefei, 230026, P. R. China

^dSchool of Chemical Engineering, Hefei University of Technology, Hefei, 230009, P. R. China

† Electronic supplementary information (ESI) available: See DOI: 10.1039/c1jm12798e

controlling the species, weight ratios, and particle sizes. In addition to the synthetic fabrication of rattle nanostructures, the catalytic activities of the nanocomposites were elucidated by using catalytic reduction of 4-nitrophenol and Suzuki coupling reaction as the examples.

2. Experimental section

Materials

Ferric chloride hexahydrate ($\text{FeCl}_3 \cdot 6\text{H}_2\text{O}$), ferric nitrate nonahydrate ($\text{Fe}(\text{NO}_3)_3 \cdot 9\text{H}_2\text{O}$), copper nitrate trihydrate ($\text{Cu}(\text{NO}_3)_2 \cdot 3\text{H}_2\text{O}$), sodium citrate, urea, polyacrylamide (PAM), potassium chloropalladite (K_2PdCl_4), silver nitrate (AgNO_3), potassium tetrachloroaurate(III) hydrate (KAuCl_4), sodium borohydride (NaBH_4), and 4-nitrophenol (4-NP) are of analytical grade and purchased from Sinopharm Chemical Reagent Co, Ltd. All reagents were used as received without further purification. Deionized water was used for all experiments.

Synthesis of $\text{Pd}@Fe_3O_4$ microspheres with rattle type nanostructure

In a typical synthesis, 0.75 mmol $\text{FeCl}_3 \cdot 6\text{H}_2\text{O}$, 2 mmol sodium citrate, 3 mmol urea, 0.15 g PAM were dissolved in 20 mL distilled water. Then, a certain amount of K_2PdCl_4 was added under vigorous stirring until it was totally dissolved. After an hour, the solution was transferred to a Teflon-lined stainless-steel autoclave (25 mL volume) and then sealed to heat at 200 °C. After a 12 h reaction period, the autoclave was cooled to room temperature. The obtained spheres were washed with water and ethanol, and then dried under vacuum to form a black powder. In this synthesis, the final products which are synthesized under different K_2PdCl_4 concentration of 0, 5×10^{-4} M, 2×10^{-3} M, 4×10^{-3} M, and 6×10^{-3} M are defined as $\text{Pd}@Fe_3O_4$ -0, $\text{Pd}@Fe_3O_4$ -1, $\text{Pd}@Fe_3O_4$ -2, $\text{Pd}@Fe_3O_4$ -3, and $\text{Pd}@Fe_3O_4$ -4, respectively. Moreover, the synthetic procedure of the $\text{Au}/\text{Fe}_3\text{O}_4$ hollow spheres is similar to the $\text{Pd}@Fe_3O_4$ except for substituting the K_2PdCl_4 with KAuCl_4 (5×10^{-3} M).

Synthesis of $\text{Ag}@Fe_3O_4$ microspheres with rattle type nanostructure

In a typical synthesis, 0.75 mmol $\text{Fe}(\text{NO}_3)_3 \cdot 9\text{H}_2\text{O}$, 3 mmol sodium citrate, 3 mmol urea, 0.15 g PAM were dissolved in 15 mL distilled water. Then, an aqueous solution of AgNO_3 (5 mL) was added under vigorous stirring. After an hour, the solution was transferred to a Teflon-lined stainless-steel autoclave (25 mL volume) and then sealed to heat at 200 °C. After a 12 h reaction period, the autoclave was cooled to room temperature. The obtained spheres were washed with water and ethanol, and then dried under vacuum for 12 h. In this synthesis, the final products which are synthesized under different AgNO_3 concentrations of 5×10^{-3} M and 2.5×10^{-2} are defined as $\text{Ag}@Fe_3O_4$ -1 and $\text{Ag}@Fe_3O_4$ -2, respectively.

The catalytic reduction of 4-nitrophenol

$\text{Ag}@Fe_3O_4$ -2 (1 mg) were added into a solution with 4-NP (5×10^{-5} mol L^{-1}) and incubated with 30 min. After that, an aqueous

solution of NaBH_4 (3.2×10^{-2} mol L^{-1}) was rapidly injected at room temperature with stirring. The color of the mixture gradually faded, indicating the reduction of the 4-NP dye. Changes in the concentration of 4-NP were monitored by examining the variations in the maximal UV/vis absorption at 400 nm. After the catalytic reaction was completed, the nanocatalysts were separated by magnetic field and rinsed by water and ethanol for 3 times for the following recycling reaction.

Suzuki cross-coupling reaction

$\text{Pd}@Fe_3O_4$ rattle particles, phenylboronic acid (1.5 mmol), sodium carbonate (2.0 mmol) were placed in an oven-dried 20 ml Schlenk-tube. The reaction vessel was evacuated and filled with argon for three times. Then iodobenzene (1 mmol) and DMF: H_2O (20 : 1, 5 mL) were added with a syringe under a counter flow of argon. The vessel was sealed and stirred at 80 °C for 8 h. Upon completion of the reaction, the mixture was cooled to room temperature and diluted with ethyl acetate (20 mL). Gas chromatography yields were determined with the use of 1,3-dimethoxybenzene (1 mmol) as an internal standard. The nanocatalysts were magnetically separated and washed by ethyl acetate and ethanol three times for the recycling experiments. In order to compare the catalytic activity of the $\text{Pd}@Fe_3O_4$ -3 and $\text{Pd}@Fe_3O_4$ -2, the Suzuki cross-coupling reactions were conducted under the same amount of Pd species.

Characterization

X-ray powder diffraction patterns (XRD) of the products were obtained on a Bruker D8 Advance diffractometer equipped with graphite monochromatized Cu-K α radiation ($\lambda = 1.5406$ Å). Transmission electron microscopy (TEM) photographs were taken on a FEI CM120 microscope and at an accelerating voltage of 120 kV and a high-resolution transmission electron microscope (HRTEM, Tecnai Model JEOL-2100 and JEOL-2010) at an accelerating voltage of 200 kV. The field emission scanning electron microscopy (FE-SEM) images were taken on a JEOL JSM-6700F SEM. Their magnetic properties (M - H curve) were measured at room temperature on a MPMS XL magnetometer made by Quantum Design Corp. The nitrogen (N_2) adsorption/desorption isotherms at about 77 K were studied depending Micromeritics, ASAP 2020M system.

3. Results and discussion

At the beginning of the experiment, an aqueous mixture of Fe(III) ions, sodium citrate, urea, polyacrylamide (PAM) and noble metal ions was prepared. After a hydrothermal treatment, rattle type nanocomposites were obtained. When K_2PdCl_4 was used as the precursor in the reaction, the product was the rattle type $\text{Pd}@Fe_3O_4$ nanocomposite. A panoramic view reveals that the as-prepared products consist of uniform spherical particles without any impurities (Fig. 1a). The average size of the microspheres is approximately 300 nm, and they are free of surface cracks and intersphere adherence. Interestingly, some broken particles can be found in the sample, which indicate that the as-prepared microspheres render a hollow nanostructure (the inset of Fig. 1a). The collapse of the hollow spheres may be caused by the high power sonication during the rinse process. The hollow

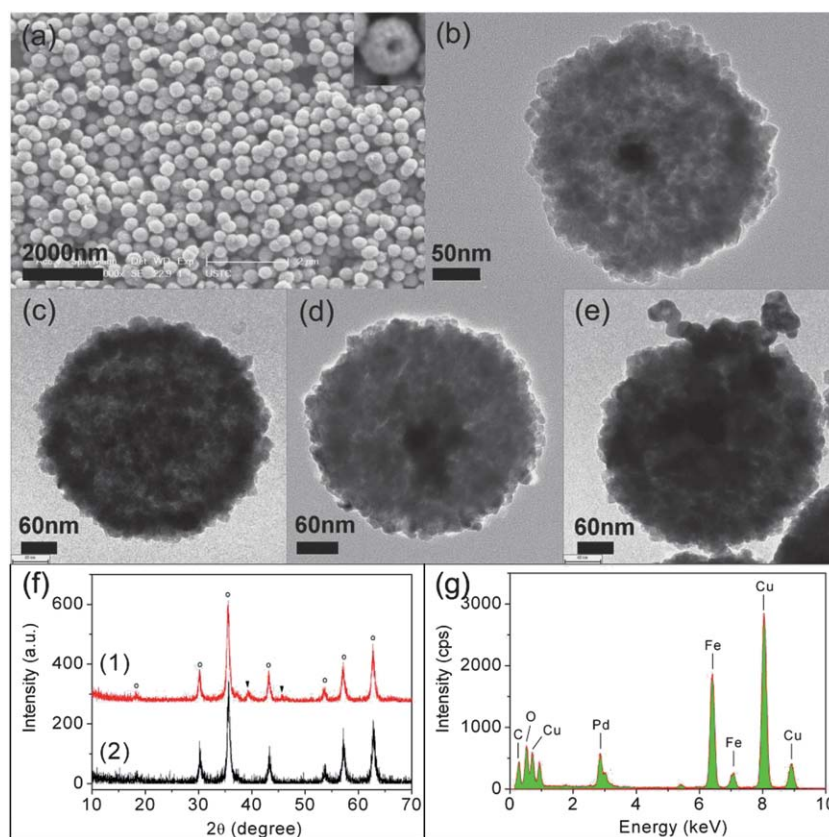


Fig. 1 SEM and TEM images of the rattle type Pd@Fe₃O₄ nanocomposites (a,b,d,e) and Fe₃O₄ hollow spheres (c); XRD patterns of the rattle type Pd@Fe₃O₄ nanocomposites (f1) and Fe₃O₄ hollow spheres (f2); EDX spectra of the rattle type Pd@Fe₃O₄ nanocomposites (g); Inset of (a) shows the SEM image of a typical broken rattle type Pd@Fe₃O₄ microsphere.

interior of the as-prepared samples is further elucidated by TEM. As shown in Fig. 1b, the inner cavity is clearly revealed by the contrast between shell and hollow interior. The shell thickness is about 40 nm and the surface is relatively rough which indicate that the shell is composed of tiny primary nanocrystals. Surprisingly, there is a small black dot (20 nm) existed in the interior of the hollow sphere, which suggests that the as-prepared microsphere shows a rattle type nanostructure.

Fig. 1f(1) shows the XRD pattern of the rattle particles, wherein all the strong peaks can be indexed to the face-centered-cubic phase of Fe₃O₄ (JCPDS no. 19-0629). Besides the peaks for Fe₃O₄, two small peaks located in 40.1° and 46.6° are found, indicating the presence of Pd nanoparticles (JCPDS no. 05-0681). The broad nature of the diffraction peaks demonstrates the Fe₃O₄ and Pd are in nanosize and the grain sizes are 10–15 nm and 6–10 nm, which agreed well with the TEM analysis. The energy-dispersive X-ray spectroscopy (EDS) analysis of the rattle nanostructure indicates the presence of Fe, Pd and O elements, proving the formation of Fe₃O₄ and Pd (Fig. 1g). The signals of Cu and C in the EDS spectrum originate from the carbon-coated copper grid. In this analysis, no Pd signal is found when the EDS is focused on the Fe₃O₄ shell (Figure SI 1a).[†] Therefore, the black dot in the Fe₃O₄ hollow sphere is believed to be Pd nanoparticle (Figure SI 1b) and the weight ratio of the Pd contents is about 6.6 wt% through elemental analysis.[†]

The weight ratio of the Pd nanoparticles located in the rattle particles can be controlled by varying the K₂PdCl₄

concentrations. When no K₂PdCl₄ was added to the starting solution, only pure Fe₃O₄ hollow spheres were obtained as the final product (Fig. 1c and Figure SI 2) (defined as Pd@Fe₃O₄-0).[†] When the K₂PdCl₄ concentration increases to 5 × 10⁻⁴ M, only a small part of the particles show a rattle type nanostructure (Figure SI 3b) and most of them are hollow spheres (defined as Pd@Fe₃O₄-1, Figure SI 3a).[†] Figure SI 4 shows the TEM image of the Pd@Fe₃O₄ composites which were prepared with 2 × 10⁻³ M K₂PdCl₄.[†] In this case, most of the particles render the encapsulated core and show the rattle type nanostructure (Fig. 1b) (defined as Pd@Fe₃O₄-2). With an increase of the K₂PdCl₄ concentration (4 × 10⁻³ M), the number of Pd nanoparticles in the hollow sphere increases (Fig. 1d and Figure SI 5, defined as Pd@Fe₃O₄-3). As shown in Figure SI 5a,[†] the Pd nanoparticles are aggregated to form rod and sphere like cores. With a further increase of the K₂PdCl₄ concentration to 6 × 10⁻³ M, more Pd nanoparticles are found in the hollow sphere (defined as Pd@Fe₃O₄-4). Unfortunately, the Pd cores cannot be well encapsulated within the rattles and most of them grow out of the hollow spheres (Fig. 1e). Moreover, it is also noticeable that some particles are terribly agglomerated by the coalescence of the outer shells (Figure SI 6a).[†]

The present approach also permits other types of synthetic architecture. For example, when AgNO₃ was employed as the precursor, Ag@Fe₃O₄ rattle particles were obtained. Fig. 2a shows the TEM image of the product which was prepared with 5 × 10⁻³ M AgNO₃. The particle is spherical and the average size

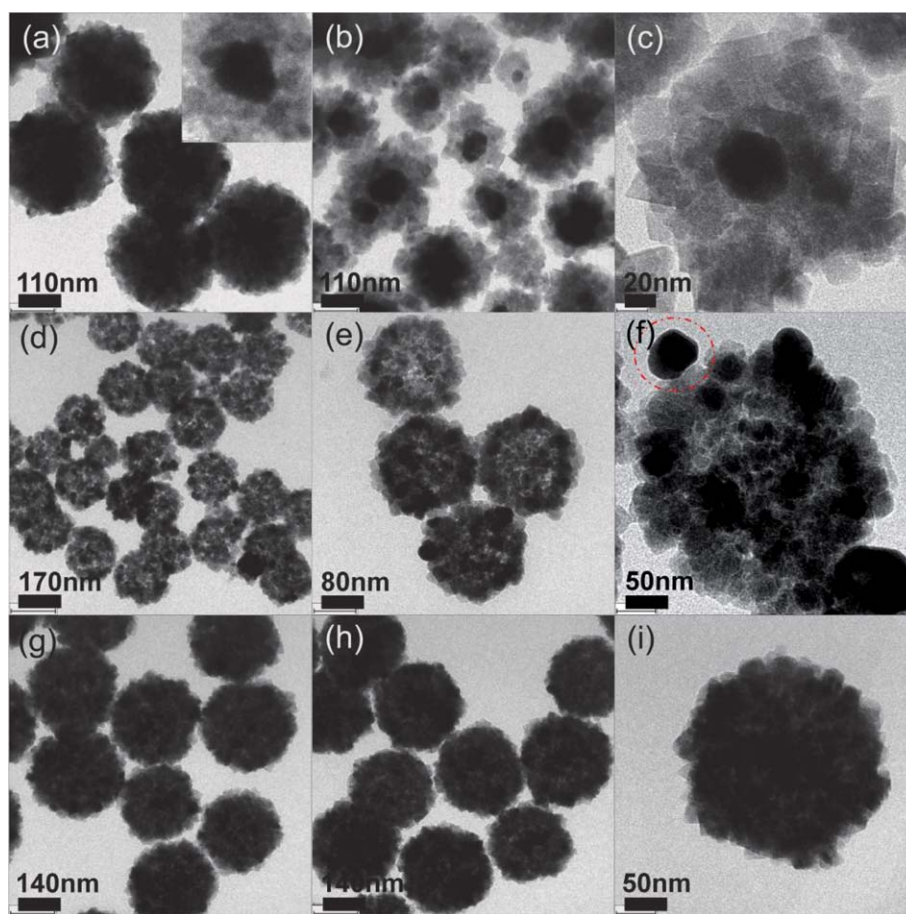


Fig. 2 TEM images of the rattle type Ag@Fe₃O₄ nanocomposites with different AgNO₃ concentrations: 5×10^{-3} M (a) and 2.5×10^{-2} M (b,c); TEM images of the Au/Fe₃O₄ nanocomposites (d,e,f); and TEM images of the Cu_{0.1}/Cu_{0.3}Fe_{2.7}O₄ nanocomposites (g) and Cu_{0.3}Fe_{2.7}O₄ hollow spheres (h,i).

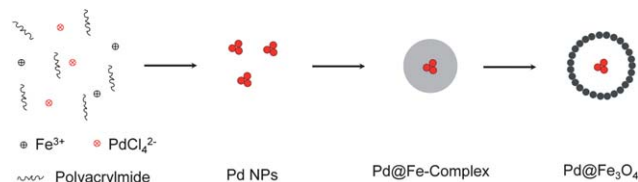
is about 300 nm. Notably, there is an Ag core located within the center of the Fe₃O₄ microspheres (inset of Fig. 2a), which agrees well with the XRD and EDS analysis (Figures SI 7 and 8).[†] It should be noticed that Fe(NO₃)₃ is used as the Fe precursor during the synthesis of Ag@Fe₃O₄ rattle particles, because large AgCl precipitates are usually obtained when FeCl₃ is used during the preparation of the precursor solutions and the large AgCl precipitates are harmful to the final product. In contrast to the Pd@Fe₃O₄, the size of the Ag@Fe₃O₄ rattle particles decreases with increasing of the AgNO₃ concentration. As shown in Fig. 2b, the average size of the Ag@Fe₃O₄ rattle particles is about 200 nm when the AgNO₃ concentration increases to 2.5×10^{-2} M. Clearly, all the Ag cores are well encapsulated with the Fe₃O₄ shells and the shells consist of many small nanograins (Fig. 2c). Here, Au/Fe₃O₄ nanocomposites also can be synthesized by using this method. Somewhat unexpectedly, the Au nanoparticles are attached on the surface rather than encapsulated in the Fe₃O₄ hollow spheres (Fig. 2d, e, f and SI9).[†] The average size of the Au/Fe₃O₄ composite hollow spheres and the Au nanoparticles are 200 and 50 nm, respectively. An increase of the KAuCl₄ concentration does not influence the size of the whole particles (data not shown). Cu(II) ions can also be used to substitute K₂PdCl₄ for the synthesis of Cu-based magnetic nanocomposites. Fig. 2g shows the TEM image of the as-prepared samples. It is found the materials are composed of well

dispersed microspheres with a typical hollow nature. From the XRD patterns (Figure SI 10a),[†] Cu materials are existed in the sample. However, due to their low contrast under the electron beam, it is very difficult to distinct the Cu nanoparticles. By soaking these particles in ammonium solution overnight, magnetic hollow spheres are achieved. The XRD analysis also demonstrates that the Cu nanoparticles are dissolved during this process (Figure SI 10b).[†] The morphologies of the samples before and after the Cu dissolving are very similar (Fig. 2g, h). Thus, the Cu nanoparticles are believed to be encapsulated in the hollow spheres. The EDS spectrum of dissolved hollow spheres is presented in Figure SI 11 (nickel grids were used as the supporter during the TEM and EDS analyses), which indicate that the final product is Cu-doped Fe₃O₄ (Cu_{0.3}Fe_{2.7}O₄) ferrite hollow spheres.[†] Therefore, the magnetic hollow spheres encapsulated with Cu nanocomposites are Cu_{0.1}/Cu_{0.3}Fe_{2.7}O₄ (Figure SI 12).[†] In this case, the weight ratio of Cu nanoparticles also increases with increasing concentration of the Cu(II). However, when the [Cu²⁺] is larger than 2×10^{-2} M, non-magnetic Fe₂O₃ impurities are existed in the final product (Figure SI 13,14).[†]

Ostwald ripening is commonly used to create hollow structures through controlled reactions.^{29,30} In the case of this rattle particle, the synthetic strategy is designed on the basis of the *in situ* reduction of Pd nanoparticle and the following transformation of Fe₃O₄ hollow spheres from Fe-Complex precursor

(Scheme 1). To test the above conceptual schemes, we conducted series of time-dependent experiments. After a 1 h hydrothermal reaction, Pd nanoparticles were formed (data not shown). These nanoparticles are acted as the cores during the formation of the Fe-Complex shell, which is cooperated by the Fe(III) ions, sodium citrate, and polyacrylamide. Thus, Pd@Fe-Complex microspheres with core/shell like nanostructure were obtained when the reaction was conducted after 4 h (Figure SI 15a).[†] In the following stage (8 h), the amorphous Fe-Complex started to crystallize and produced Fe₃O₄ nanograins on the surface of the core shell microspheres (Figure SI 15b). As a result, the Pd@Fe-Complex microspheres experienced the well known Ostwald ripening process and transform to Pd@Fe₃O₄ rattle particles (Figure SI 15c).^{†25} With an increase of the K₂PdCl₄ concentration, the number of the Pd nanoparticles increase and then the Pd nanoparticles aggregate to reduce their surface energy. Thus, the Pd@Fe₃O₄ rattle particles which were synthesized under a high K₂PdCl₄ concentration often rendered a larger number of the Pd nanoparticles. For the Ag@Fe₃O₄ composite particles, the average size of the as-formed Ag is very large (60–120 nm) and they are very stable in the solution. Therefore, the Ag@Fe₃O₄ often shows a single core/single shell nanostructure. With increasing of the Ag(I) concentration, the individual core numbers increase. Then the shell thickness decreases and further leads to a decrease of the size of the whole particle.

The formation of these rattle particles are composed of three major processes in the sealed system: 1) formation of metallic cores; 2) coating the metallic cores with amorphous Fe-Complex; 3) evacuation of interior amorphous Fe-Complex to form hollow Fe₃O₄ by Ostwald ripening. Firstly, the metallic ions are very easily to be reduced to form noble nanoparticles under the high temperature reaction. The as-formed metallic cores are small in size and can be well dispersed in the reaction system due to the presence of polyacrylamide polymer. These nano-cores are reactive, which may catalyze the formation of the Fe-Complex and leads to *in situ* deposition of Fe-Complex products around the metallic nanoparticles surface to form core shell like nanostructure. The affinity between the metallic core and the Fe-Complex is critical in this process. When the KAuCl₄ precursor was employed, the Au nanoparticles prefer to attach on the surface of the Fe₃O₄ particles rather than encapsulated within the hollow interior. Although the real reason is not very clear, it is believed that the affinity between Au and the Fe-Complex is weak and the Fe-Complex cannot coat the Au nanoparticles to form core shell nanostructure. With further increasing of the reaction time, the amorphous Fe-Complex starts crystallizing at the surface of the particles. Meanwhile, some interior space would be generated owing to inhomogeneous distribution of



Scheme 1 Schematic illustration of the formation of the rattle type nanostructure.

crystallites within the Fe-Complex shell. The inner amorphous Fe-Complex undergoes mass relocation through dissolving and recrystallized on the exterior of the particles. Finally, the rattle particles are obtained.

The rattle type Pd@Fe₃O₄ particles show a porosity nature which can be substantiated by the measurement of nitrogen adsorption-desorption isotherms and the Brunauer–Emmett–Teller (BET) surface area. As shown in Fig. 3, the isotherm can be classified as type IV with an apparent hysteresis loop in the range 0.45–1.0 P/P₀, indicating the presence of mesopores. The BET surface area of the Pd@Fe₃O₄ rattle particles (Fig. 1a,b) is 31.44 m² g⁻¹. This value is higher than the single crystallized Fe₃O₄ indicating that the present Fe₃O₄ shell may be porous wherein the mesoporous can be attributed to the interspaces of the aggregated Fe₃O₄ nanograins.³¹ Fig. 4 shows the hysteresis loop of typical Pd@Fe₃O₄ rattle particles measured by sweeping the external field between -0.8 to 0.8 T at room temperature. No obvious remanence or coercivity is observed in the magnetization curve at room temperature, suggesting the superparamagnetic character. The saturated mass magnetization is estimated to be 67.6 emu/g and this value is much higher than the previously reported magnetic nanocatalysts, which enable the as-prepared nanocatalysts can be separated from the reaction system very quickly.^{15,16}

With permeable outer shell, functional and tunable core, and superparamagnetic property, the as-prepared rattle particles are expected to be widely applied in magnetic separable nanocatalysts. Initially, the reduction of 4-nitrophenol (4-NP) by NaBH₄ was used as a model reaction to characterize the performance of the 200 nm Ag@Fe₃O₄ catalyst system. Without the Ag catalyst, the reduction does not proceed. When the Ag@Fe₃O₄ catalyst was introduced into the solution, the color of the solution faded gradually, indicating the reduction of 4-NP proceeded. The chosen catalysts were 200 nm Ag@Fe₃O₄ with 60 nm Ag core, with a high Ag weight ratio. The kinetics of the 4-NP reduction in presence of NaBH₄ was studied by UV-vis spectroscopy. Fig. 5 shows the UV-vis spectra for the reduction of 4-NP measured at a different time during the progress of the reaction. After the addition of Ag@Fe₃O₄, it was found that the peak height at 400 gradually decreases with time. The decrease of

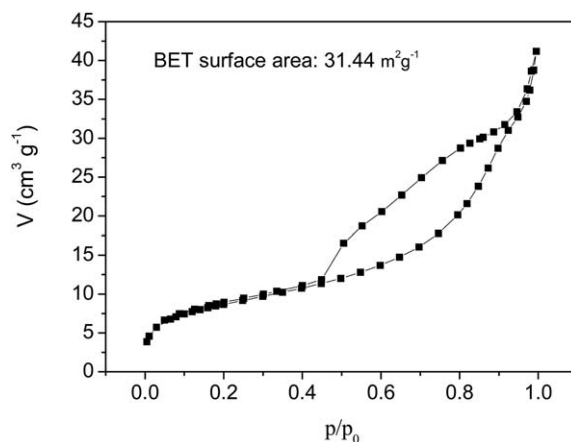


Fig. 3 Nitrogen adsorption-desorption isotherm of the as prepared Pd@Fe₃O₄-2 rattle particles.

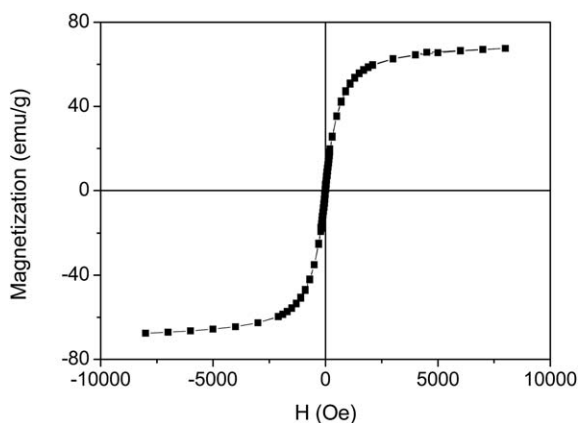


Fig. 4 $M-H$ (b) curve of the as prepared Pd@Fe₃O₄-2 rattle particles.

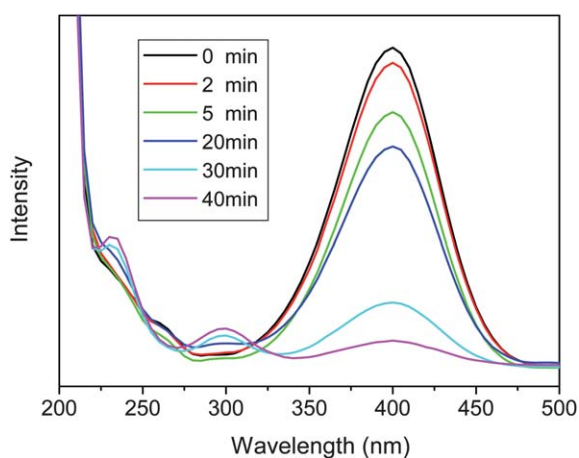


Fig. 5 Time-dependent UV-vis absorption spectral changes of the reaction mixture catalyzed by 200 nm Ag@Fe₃O₄ nanocatalyst.

peak intensity at 400 nm with time can be taken into account to calculate the rate constant. The linear relationship of $\ln(C_t/C_0)$ versus time was observed, indicating that the reactions followed first-order kinetics. The observed rate constant for the catalyst was $8 \times 10^{-4} \text{ s}^{-1}$ calculated directly from the slope of the straight line in Fig. 6. After the completion of the reaction, these nanocatalysts can be separated from the solution by a magnet. The Ag@Fe₃O₄ can be at least reused for 5 times and keep about 85% of their catalytic activity. The catalytic activity of Pd@Fe₃O₄ rattle particles was tested for the Suzuki cross-coupling reaction. For Pd@Fe₃O₄-2, the coupling product was obtained with 98% of the isolated yield after 8 h of the reaction shown in Table SII. However, when the Pd@Fe₃O₄-3 was used for this coupling reaction under the same conditions, the Suzuki cross-coupling product with 82% conversion yield was detected. The Pd nanoparticles encapsulated within Pd@Fe₃O₄-3 are aggregated and show a large variation. It is reported that the catalytic activity of the aggregated Pd nanoparticles is lower than the monodispersed ones.³² Thus the Pd@Fe₃O₄-2 exhibits a higher catalytic property than the Pd@Fe₃O₄-3. Although the catalytic reactivity of the rattles are not as high as the naked Pd nanoparticles, which must be due to the presence of polyacrylamide on the surface of the Pd core, the Pd cores are very stable during the catalytic reaction

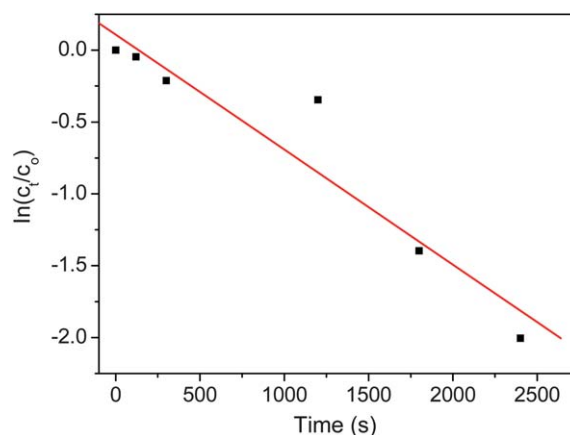


Fig. 6 The relative Plot of $\ln(C_t/C_0)$ versus time with Ag@Fe₃O₄ catalysts.

and they can be separated by only applying a small magnet nearby the reaction system. Therefore, the as-prepared rattle type particles can be used as reusable catalysts with high catalytic activity, proving that the Fe₃O₄ shell can maintain a stable metal core while allows the diffusion of small active molecules in and out the nanoreactors.

4. Conclusion

In summary, a facile strategy has been demonstrated for preparation of rattle type noble metal@Fe₃O₄ nanocomposites with uniform morphology, tunable sizes, and controllable species and weight ratios. The construction of such particles is achieved in a one-step process, which is on the basis of the *in situ* reduction of noble metal nanoparticle and the following transformation of Fe₃O₄ hollow spheres from Fe-Complex precursor through an Ostwald ripening process. These rattle nanostructures are ideal recyclable catalysts for liquid-phase reactions because they contain superparamagnetic components for efficient magnetic separation and a porous Fe₃O₄ shell for stabilization of the encapsulated catalyst particles. These particles were successfully applied in the catalytic reduction of 4-nitrophenol and Suzuki cross-coupling reaction. In addition, this strategy can be extended to fabricate hollow Fe₃O₄ microspheres with other cores in a facile and scalable way.

Acknowledgements

This work was supported by “the Fundamental Research Funds for the Central Universities, No.WK2090000002” and a grant from the University Grants Committee of HKSAR (Area of Excellence Scheme AoE/P-03/08).

Reference

- 1 X. W. Lou, L. A. Archer and Z. C. Yang, *Adv. Mater.*, 2008, **20**, 3987.
- 2 S. W. Kim, M. Kim, W. Y. Lee and T. Hyeon, *J. Am. Chem. Soc.*, 2002, **124**, 7642.
- 3 F. Caruso, R. A. Caruso and H. Mohwald, *Science*, 1998, **282**, 1111.
- 4 C. I. Zoldesi and A. Imhof, *Adv. Mater.*, 2005, **17**, 924.
- 5 J. Li and H. C. Zeng, *Angew. Chem., Int. Ed.*, 2005, **44**, 4342.
- 6 S. H. Wu, C. T. Tseng, Y. S. Lin, C. H. Lin, Y. Hung and C. Y. Mou, *J. Mater. Chem.*, 2011, **21**, 789.

- 7 H. X. Li, Z. F. Bian, J. Zhu, D. Q. Zhang, G. S. Li, Y. N. Huo, H. Li and Y. F. Lu, *J. Am. Chem. Soc.*, 2007, **129**, 8406.
- 8 K. Kamata, Y. Lu and Y. Xia, *J. Am. Chem. Soc.*, 2003, **125**, 2384.
- 9 J. Y. Kim, S. B. Yoon and J. S. Yu, *Chem. Commun.*, 2003, 790.
- 10 Y. Yin, R. M. Rioux, C. K. Erdonmez, S. Hughes, G. A. Somorjai and A. P. Alivisatos, *Science*, 2004, **304**, 711.
- 11 J. G. Lee, J. C. Park, J. U. Bang and H. J. Song, *Chem. Mater.*, 2008, **20**, 5839.
- 12 J. C. Park, J. Y. Kim, E. J. Heo, K. H. Park and H. Song, *Langmuir*, 2010, **26**, 16469.
- 13 X. J. Wu and D. S. Xu, *J. Am. Chem. Soc.*, 2009, **131**, 2774.
- 14 L. F. Tan, D. Chen, H. Y. Liu and F. Q. Tang, *Adv. Mater.*, 2010, **22**, 4885.
- 15 D. K. Yi, S. S. Lee and J. Y. Ying, *Chem. Mater.*, 2006, **18**, 2459.
- 16 S. H. Xuan, Y.-X. J. Wang, J. C. Yu and K. C.-F. Leung, *Langmuir*, 2009, **25**, 11835.
- 17 J. P. Ge, Q. Zhang, T. R. Zhang and Y. D. Yin, *Angew. Chem., Int. Ed.*, 2008, **47**, 8924.
- 18 Y. H. Deng, Y. Cai, Z. K. Sun, J. Liu, C. Liu, J. Wei, W. Li, C. Liu, Y. Wang and D. Y. Zhao, *J. Am. Chem. Soc.*, 2010, **132**, 8466.
- 19 S. H. Li, E. B. Wang, C. H. Tian, B. D. Mao, Z. H. Kang, Q. Y. Li and G. Y. Sun, *J. Solid State Chem.*, 2008, **181**, 1650.
- 20 P. Jin, Q. W. Chen, L. Q. Hao, R. F. Tian, L. X. Zhang and L. Wang, *J. Phys. Chem. B*, 2004, **108**, 6311.
- 21 J. Liu, S. Z. Qiao, Q. H. Hu and G. Q. Lu, *Small*, 2011, **7**, 425.
- 22 Q. L. Fang, S. H. Xuan, W. Q. Jiang and X. L. Gong, *Adv. Funct. Mater.*, 2011, **21**, 1902.
- 23 H. C. Zeng, *J. Mater. Chem.*, 2006, **16**, 649.
- 24 X. W. Lou, Y. Wang, C. L. Yuan, J. Y. Lee and L. A. Archer, *Adv. Mater.*, 2006, **18**, 2325.
- 25 W. Cheng, K. B. Tang, Y. X. Qi, J. Sheng and Z. P. Liu, *J. Mater. Chem.*, 2010, **20**, 1799.
- 26 J. Liu, S. Z. Qiao, S. B. Hartono and G. Q. Lu, *Angew. Chem., Int. Ed.*, 2010, **49**, 4981.
- 27 J. Liu, R. Harrison, J. Z. Zhou, T. T. Liu, C. Z. Yu, G. Q. Lu, S. Z. Qiao and Z. P. Xu, *J. Mater. Chem.*, 2011, **21**, 10641.
- 28 J. S. Chen, C. P. Chen, J. Liu, R. Xu, S. Z. Qiao and X. W. Lou, *Chem. Commun.*, 2011, **47**, 2631.
- 29 M. K. Devaraju, S. L. Yin and T. Sato, *Cryst. Growth Des.*, 2009, **9**, 2944.
- 30 B. Liu and H. C. Zeng, *Small*, 2005, **1**, 566.
- 31 L. P. Zhu, H. M. Xiao, W. D. Zhang, G. Yang and S. Y. Fu, *Cryst. Growth Des.*, 2008, **8**, 957.
- 32 B. H. Yoon and C. M. Wai, *J. Am. Chem. Soc.*, 2005, **127**, 17174.